Cyclic Testing of Concrete-Filled Circular Steel Bridge Piers having Encased Fixed-Based Detail

Julia Marson[1] and Michel Bruneau, M.ASCE[2]

Abstract: To investigate their adequacy as energy dissipating elements during earthquakes, this paper reports on cyclic inelastic tests executed to determine the maximum strength and ductility of four concrete-filled circular steel piers joined to a foundation detail proposed to develop the full composite strength at the base of these columns. Column diameters considered were 324 and 406 mm, with D/t ratios ranging from 34 to 64. The ductility of all tested columns was found to be good, all columns being able to reach drifts of 7% before a significant loss in moment capacity occurred as a result of cracks opening on the local buckles, suggesting that concrete-filled steel tubes can be effective as bridge piers in seismic regions of North America.

DOI: 10.1061/(ASCE)1084-0702(2004)9:1(14)

CE Database subject headings: Bridge piers; Composite columns; Cyclic tests; Seismic response; Footings; Design criteria.

Introduction

According to the design philosophy prevailing in North America (AASHTO 1994; CSA 2000), bridges are designed to ensure that during an earthquake, their superstructure remains elastic while their substructure yields and behaves in a ductile manner. Currently in North America, nearly all new highway bridge substructures are constructed of reinforced concrete, even when bridges have a steel superstructure. However, in view of the growing worldwide emphasis on ductile detailing and sound earthquake resistance design, piers made from unstiffened circular steel tubes filled with concrete may be an economically viable concept worthy of consideration.

In such a composite pier, among their possible advantages: (1) the steel tube can provide some confinement of the concrete and permit development of the full composite capacity of the column, with stable seismic energy dissipation; (2) all the concrete in the member can contribute to strength and ductility of the member as concrete spalling does not occur; (3) the steel shell can act as formwork for the concrete in a concrete-filled steel column; (4) construction of the bridge may be accelerated if the steel shell alone can provide resistance to dead load; (5) the steel components can be fabricated off site in a controlled environment; (6) the concrete core delays local buckling of the steel tube, and prevents its inward buckling, also enhancing ductility of the composite columns; (7) reinforcing bars are unnecessary in the concrete; (8) there is no need for stain protection on piers when the superstructure is of weathering steel (although some protection may be necessary at the base depending on the particular detailing used, it can be accomplished easier there); and (9) the final aesthetics of a concrete-filled steel column are compatible with current bridge design practice.

The potential economical advantages of concrete-filled steel columns in tall buildings have long been recognized (Tarics 1972). In North America and Australia, concrete-filled steel columns have recently been used in some buildings (e.g., Bauer 1988; Webb and Peyton 1990), and much earlier in nonbuilding applications, as pylons for hydroelectric lines in Switzerland (Vogeli 1950), and as piles in many applications. A four level interchange was built in Almondsbury, U.K., and supported on concrete-filled steel piers (Kerensky and Dallard 1968). This suggests that filling a steel tube with concrete can be cost effective, and (if shown to have good ductile behavior) desirable to provide satisfactory seismic performance.

A literature review revealed that while a significant number of axial compression tests have been conducted, there has been far fewer flexural cyclic tests (Marson and Bruneau 2000). From the results of seven researchers who have looked at 49 circular columns subjected to both axial and bending forces, only 12 columns have been subjected to cyclic loading. Furthermore, in these studies, the largest circular concrete-filled column subjected to cyclic loading had a diameter of 320 mm and most researchers welded the base of the steel tube to a thick steel plate unrepresentative of possible field conditions.

In the above perspective, this paper reports on cyclic inelastic tests executed to determine the maximum strength and ductility of four concrete-filled circular steel tube columns, of either 324 or 407 mm in diameter, and joined to a foundation detail proposed to develop the full composite capacity at the base of these columns. Results from these experiments were also used to support the development of design equations presented in a companion paper (Bruneau and Marson 2004).

Literature Review

While considerable knowledge exists on the behavior of noncyclically loaded composite columns (Viest et al. 1997), the behavior of concrete-filled unstiffened steel tubes subjected to repeated cycles of large inelastic deformations is less understood.

[1]Project Engineer, Harmer Podolak Engineering, 221-39 Robertson Rd., Nepean ON, Canada K2H 8R2.

[2]Director, MCEER, Professor, Dept. of CSEE, Univ. at Buffalo, Buffalo, NY 14260. E-mail: bruneau@mceermail.buffalo.edu

Note. Discussion open until June 1, 2004. Separate discussions must be submitted for individual papers. To extend the closing date by one month, a written request must be filed with the ASCE Managing Editor. The manuscript for this paper was submitted for review and possible publication on June 11, 2002; approved on June 24, 2003. This paper is part of the ***Journal of Bridge Engineering***, Vol. 9, No. 1, January 1, 2004. ©ASCE, ISSN 1084-0702/2004/1-14–23/$18.00.

Boyd et al. (1995) subjected five circular composite column specimens to cyclic inelastic lateral displacements under a constant axial load. All columns had a diameter, D, of 203.2 mm and the steel shell thickness, t, was either 1.91 or 2.77 mm (for D/t ratios of 106 and 73, respectively). The footing of the column was attached to the laboratory strong floor with bolts in order to provide full base fixity. Although local buckling occurred in all of the shells, all columns exhibited stable behavior and maintained, or exceeded, the ACI 318-89 predicted load capacity at a minimum displacement ductility, μ, of 6. The presence of shear studs in some specimens reduced strength degradation at large deformations, thus slightly increasing total energy dissipation.

Other researchers considered high strength concrete. Prion and Boehme (1994) tested three specimens with 152 mm outside diameter and 1.65 mm steel shell thickness (for high D/t ratios of 92), and a concrete cylinder strength of 92 MPa. The cyclic tests demonstrated good ductility and energy dissipation of the members. Slight pinching in the hysteretic curves was observed and attributed to the opening and closing of concrete cracks while the steel tube was yielding and buckling. Fracture of the steel tube occurred on the tension side at a strain of approximately three times the yield strain. Alfawakiri (1997) tested three hot-formed seamless steel tubes, 3 mm thick and 152 mm in diameter, filled with 72 or 90 MPa high strength concrete. The beam columns were each welded to a thick steel base plate strengthened and made more rigid by adding two stiffeners to achieve a fixed base connection. These flexible specimens reached drift in excess of 7%; testing stopped after the specimens exhibited significant local buckling, strength degradation, or fracture on a local buckle.

Kitada (1992) summarized some of the Japanese research on this topic and showed that the circular cross section is better suited than the rectangular cross section to sustain, in a ductile manner, numerous cycles of bending, or shear under constant compression.

In the above tests, the lateral force–displacement curve obtained under monotonic loading for concrete-filled steel columns was reported to provide an envelope for the behavior expected under cyclic loading. Stiffness degradation was, typically, observed upon repeated load reversals, but little degradation of ultimate strength occurred up to high ductility.

The largest circular concrete-filled column subjected to cyclic loading in the above tests had a diameter of 320 mm. Furthermore, most researchers welded the base of the steel tube to a thick steel plate (sometimes with thick base stiffeners) rather than providing a base connection representative of what could be constructed in the field. It also appears that the adequacy of the bond between the two materials during cyclic testing, and whether the concrete core becomes triaxially confined by the steel tube, remain contentious unresolved issues.

Design of Specimens

Full-Scale Bridges Characteristics and Analysis

To ensure that the tested specimens had characteristics and dimensions representative of real prototypes, full-scale bridges (and their piers) were designed according to the Ontario Highway Bridge Design Code (MTO 1991) and the Canadian Highway Bridge Design Code (CSA 2000). A total of 1296 bridges were designed using a suite of different configurations, geometries, and parameters likely to be encountered in highway bridges situated in North America. All bridges considered were overpasses carrying bidirectional traffic and running perpendicular over a divided highway. The superstructure of all bridges was designed as a two

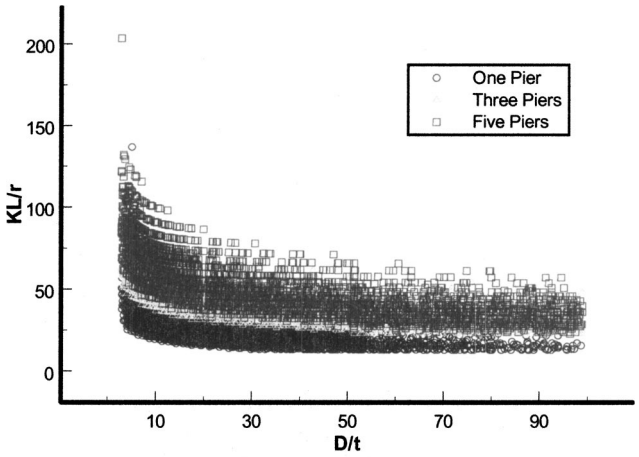

Fig. 1. Prototype designs (one pier, three piers, and five piers bents)

span slab-on-girder bridge. The slab consisted of a 50 mm wearing surface and a 250 mm reinforced concrete deck slab. Concrete traffic barriers and sidewalk allowances were designed for both sides of the bridge. The girders were steel I sections readily available through Canadian mills and placed at a center-to-center spacing of approximately 2 m. In this parametric design study:

- bridges were simply supported or continuous over pier bent;
- bridges had 2, 4, or 6 traffic lanes;
- individual spans had to accommodate an underpass highway of 1, 2, or 3 traffic lanes;
- pier heights were 5, 6, or 8 m;
- pier bents had 1, 3, or 5 piers;
- soil was profile I ($S=1.0$) or profile IV ($S=2.0$) per CSA 2000; and
- zonal acceleration ratios, A, were 0.15 (Shawinigan, Que.), 0.2 (Ottawa, Ont.), 0.3 (Vancouver, B.C.), and 0.4 (Victoria, B.C.).

The CAN/CSA-S16.1-M94 standard (CSA 1994) was used for the design of the concrete-filled steel pier (due to lack of such provisions in the Canadian bridge codes). Seismic response modification factors, R, of 3.0 for single column bents and 5.0 for multicolumn bents were used.

Fig. 1 summarizes all the resulting full-scale piers that were designed. It is observed that many pier sizes could be used for more than one design. In addition to the criterion of bridge applicability, the following was also considered to select the four test pier specimens.

The D/t ratio, which relates to the local buckling resistance of hollow circular flexural members, was retained as a first parameter of significance. According to CAN/CSA.S16.1-M94 (CSA 1994), a circular hollow section of yield strength 350 MPa with a D/t ratio less than 37 is a class 1 section [i.e., defined by CSA.S16.1-M94 (CSA 1994) as capable of sustained plastic rotation after reaching the plastic moment M_p], a D/t ratio less than 51 is a class 2 section (i.e., defined as able to reach M_p but unable to sustain large plastic rotation thereafter), and a D/t ratio less than 67 is a class 3 section (i.e., defined as only able to reach the yield moment M_y). Specimens with D/t values near those limits were desired. For comparison, the AASHTO LRFD bridge design specifications prescribe a limit of 47 for compact concrete-filled tubes. The AISC LRFD provisions specify a limit of 40 for compact hollow tubes, and of 26 in seismic applications.

From the results in Fig. 1, and knowledge from Knowles and Park (1969) that a slenderness ratio, kL/r_c less than 35 is required to ensure confinement of the concrete fill, the following desired

D/t and kL/r_c ratio values were deemed desirable for the test specimen characteristics:

1. $D/t=34$ and $kL/r_c=30$ (single pier bent) or 60 (multiple piers bent).
2. $D/t=51$ and $kL/r_c=30$ (single pier bent) or 60 (multiple piers bent).
3. $D/t=51$ and $kL/r_c=22$ (single pier bent) or 44 (multiple piers bent).
4. $D/t=64$ and $kL/r_c=22$ (single pier bent) or 44 (multiple piers bent).

[k taken as 1.0 per CAN/CSA S16.1-M94 (CSA 1994) since $P-\Delta$ analyses were considered in all cases]. As shown in Fig. 1, these four columns fall within the range of possible design revealed by the parametric study for the cases of one, three and five piers per bent.

Furthermore, to ensure proper consideration of the relative magnitude of axial forces present in the prototype composite piers during earthquakes, the ratios C_f/C_r, M_f/M_r, C_f/C_{rc}, and C_r/C_{rc} were compared for the various possible prototypes to see which specimens could be tested to accommodate similar ratios. C_f and M_f are the factored axial load and moment applied to the column, respectively, and C_r, C_{rc}, and M_r are the axial resistance of the steel tube and composite cross section, and the bending resistance of the composite cross section, respectively, as defined in CAN/CSA S16.1-M94 (CSA 1994). Restrictions with the test setup also impacted selection of the test specimens. The maximum axial and horizontal loads that could be applied were 2,000 and 1,000 kN, respectively, and the maximum height of the column was restricted to 2,200 mm.

With this criteria, and using the label CFST ## where CFST refers to ''concrete-filled steel tube'' and the number ## refers to the D/t ratio of the steel tube, the following four test columns were chosen:

- CFST 51, with a 323.9 mm diameter and a 6.35 mm thickness.
- CFST 34, with a 323.9 mm diameter and a 9.53 mm thickness.
- CFST 64, with a 406.4 mm diameter and a 6.35 mm thickness.
- CFST 42, with a 406.4 mm diameter and a 9.53 mm thickness.

Note that it was originally intended to have two columns with the same D/t ratio of 51. However, the column with a D/t ratio of 51, a kL/r_c value of 30, and a 406.4 mm diameter steel tube with a steel thickness of 7.53 mm could not be obtained by the fabricators, and was substituted by specimen CFST 42.

Design of Foundation

A new foundation design concept (for application in actual bridges) was developed to provide full fixity and resist the columns' composite strength. The proposed design consists of a foundation in which the full composite flexural strength of the column is resisted by steel components welded to the steel tube and encased inside the concrete foundation. To simplify fabrication and reduce costs, all foundations were designed as if supporting specimen CFST 42, found to have the largest flexural strength. The proposed foundation design is shown in Fig. 2.

This system is described per its construction sequence. The bottom of the steel tube was welded to a 30-mm-thick bottom plate. Two C channels with their flanges pointing away from the tube were placed alongside the steel tube on either side and welded longitudinally to the bottom plate. A 10-mm-thick top plate with a hole cut out for the steel tube was then slipped over the column. The two longitudinal ends of the plate were welded to the top flange of the channels, and the transverse ends of the plate that were in contact with the flanges of the channels were also welded. The inside of the cut hole was then welded to the column.

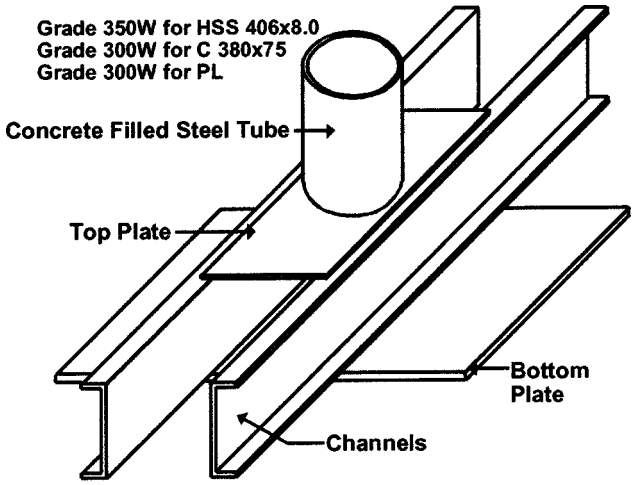

Fig. 2. Schematic of foundation connection detail

The channels and plates were used to transfer the entire composite moment from the column. The bottom plate was also used to resist the vertical tension and compression that was left in the tube when the load reached the bottom of the column. However, the moment was expected to be low on the bottom plate due to the lateral load being transferred into the top plate and channels. No reinforcing bars were needed in the concrete foundation as the structural steel members were designed to transfer all forces but some were added to accommodate the test setup as described later. Note that the same design concept could be expanded to provide resistance to the full composite strength of the column in two orthogonal directions.

Materials

Average compressive concrete cylinder strengths (on the day of testing) of 37, 40, 35, and 35 MPa for CFST 64, CFST 34, CFST 42, and CFST 51 were obtained, respectively. The steel for the column was specified Grade C A500 (specified F_y of 350 MPa), while the plates and channels were specified to be CSA G40.21 M-300W steel. The measured yield strengths of the steel tubes were 449, 415, 505, and 405 MPa for CFST 64, CFST 34, CFST 42, and CFST 51, respectively (1.16–1.44 times stronger than ordered). ASTM A500 tube tolerances on steel tube thicknesses are $\pm 10\%$. The measured steel thicknesses for the specimen (as received) were 5.5, 7.5, 9.5, and 5.5 mm for CFST 64, CFST 34, CFST 42, and CFST 51, respectively, i.e., 15, 27, 0, and 15% smaller than the specified values (ordered).

Test Setup

Tests were performed at the University of Ottawa Structures Laboratory. Three independent hydraulic MTS actuators were used for loading each specimen, two for the vertical load and one for the horizontal load. The foundation was attached to the laboratory strong floor using four high strength bolts (each 64 mm in diameter and 1,800 mm long). A horizontal loading beam was used to transfer the vertical axial load from the actuators to the column. Two existing spacers were used to connect the loading beam to the column. Fig. 3 illustrates front and side views of the test assembly.

Due to setup size restrictions, the vertical load actuators had to sit on top of the foundation during testing. Therefore, when the vertical load was applied to axially compress the specimens, the concrete foundation was subjected to uplifting tension forces

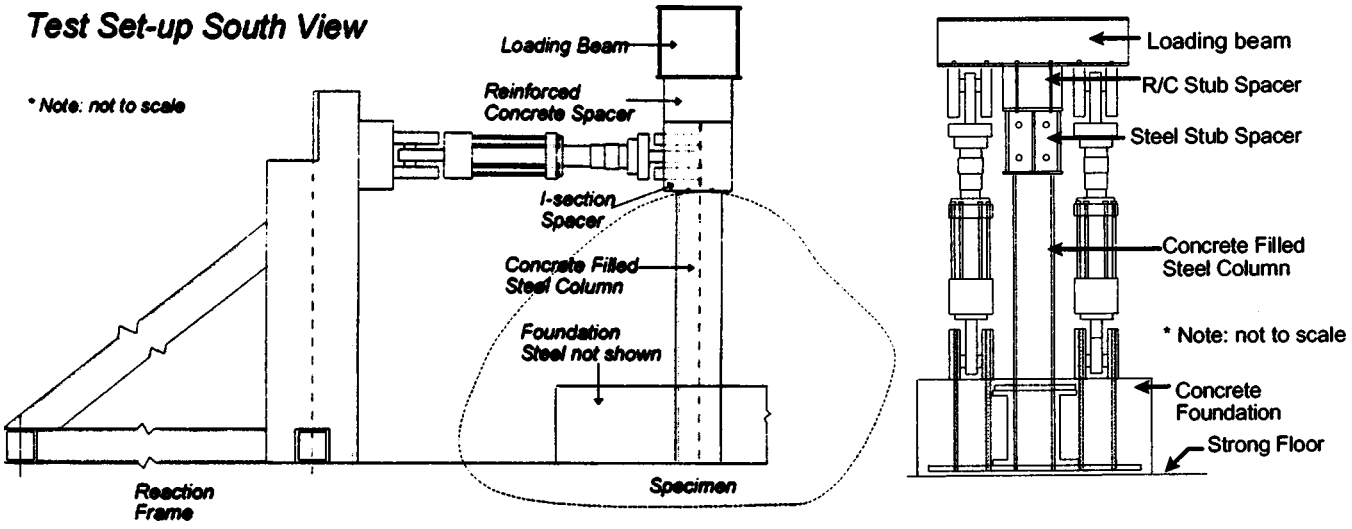

Fig. 3. Test setup

from the actuators. Because the steel tube ran the entire depth of the foundation creating an obstacle to what would have been the simplest path of reinforcement, a reinforcing cage was built around the column and through the channels to resist the forces caused by the actuators' upward pull. Concrete was poured up to 260 mm above the top plate of the embedded steel foundation system.

Four bolts running through the swivel head on the bottom of each actuator and through the entire foundation were needed to attach the vertical actuators to the foundation.

Instrumentation

Thirty-six strain gauges were installed on all specimens to allow assessments of the moment in the channels, the shear force and moment transferred from the steel tube to the top and bottom plates, and flexure and axial forces at various locations in the steel tube above and in the foundation. Low voltage displacement transducers (LVDT) were used to measure various displacements of the test setup, column displacement at midheight, and in attempts to capture the magnitude of local buckling. A temposonic displacement transducer was used to measure the column displacement at the horizontal actuator, 2,200 mm above the concrete foundation. Two other temposonic transducers measured the tip of the column displacement, approximately 1,895 mm above the concrete foundation, on the north and south side of the column, respectively, to monitor whether the column was accidently subjected to torsion during testing.

Experimental Observations

In the following, a positive force or displacement corresponds to the specimen pushed towards the east. A grid was painted on each column for reference during the test to visually facilitate observation of local buckling. Squares in the grid for columns having diameters of 406 and 323.9 mm were 50 mm×50 mm and 45 mm×45 mm, respectively.

Loading

In all tests, the axial load was first applied to the column and held constant for the duration of the test for each of the experiments. CFST 51, CFST 34, CFST 64, and CFST 42 were subjected to axial loads of 1,600, 1,920, 1,000, and 1,920 kN, respectively. The ATC-24 (ATC 1992) procedure was then followed for all tests. An effective yield displacement was found by observing the force–displacement curve as the test was progressing, and determining when significant departure from elastic response started to occur. A visual estimate of the point at which a bilinear force–displacement relationship would provide hysteretic energy equivalent to the extrapolated experimental one (based on smooth projection of acquired results) was deemed adequate to define this point as the yield displacement. For all tests, significant departure from the elastic curve occurred at approximately 1% drift. Therefore, the yield deformation was taken as 1% drift and the tests were continued using drift as the prescribed deformation instead of yield displacement.

CFST 64

Fig. 4 shows the hysteretic force–deflection results recorded. During testing, no evidence of yielding or damage could be seen until the third positive cycle at $0.75\delta_y$ when slight cracking due to separation on the tension side at the interface of the steel tube and concrete foundation could be observed. During this cycle, the strain gauges on the steel tube had not reached yield, and the force–deflection plot still appeared to be a straight line. Deformation was increased to 22 mm, corresponding to 1% drift, for the next three cycles. Many of the strain gauges on the steel tube, both in and above the foundation, reached yield in both tension and compression. The force–deflection curve begun to deviate from the straight elastic line, and supported by information from the strain gauges, it was determined that the yield point had been reached. Slight buckling on the east side of the column was observed during the second cycle at 2% drift. On reverse excursion, slight buckling was also seen on the west side but it was not as significant as the east side buckle. A maximum applied horizontal force of 164 kN was reached during the cycle at 3% drift. The buckle grew on the east side and did not completely straighten out during the negative cycle at 3% drift (Fig. 5). Pinching in the hysteretic curve was visible starting at the second cycle of 3% drift. From then onward, the buckles on both sides of the column continued to grow with the steel remaining ductile in all subsequent cycles (Fig. 5) until the first cycle at 7% drift when a large gap opened between the column and the foundation at the west side. During the negative cycle, necking started to develop

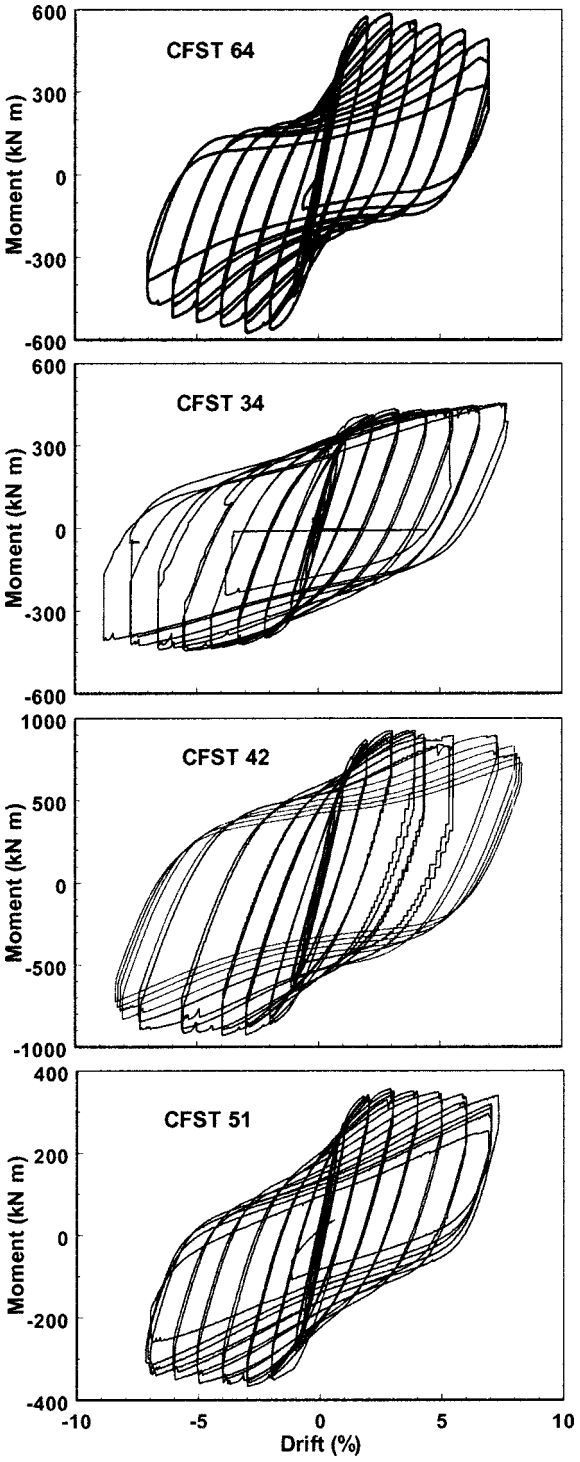

Fig. 4. Force–displacement hysteretic curves for tested specimens (common horizontal axis scale, different vertical axis scales)

through the thickness of the steel shell and cracking was observed on the east side. The crack appeared to have penetrated through the tube. A drop in strength was visible in the force–deflection curve during the second positive cycle at 7% drift. Pulverized concrete spilled out through the crack in the buckle as it opened wider. After testing stopped, the crack on the upper portion of the buckle on the west side was measured to have a length of 47 mm and a width of 3 mm while the crack on the lower portion of the buckle had a length of 195 mm and a width of 22 mm.

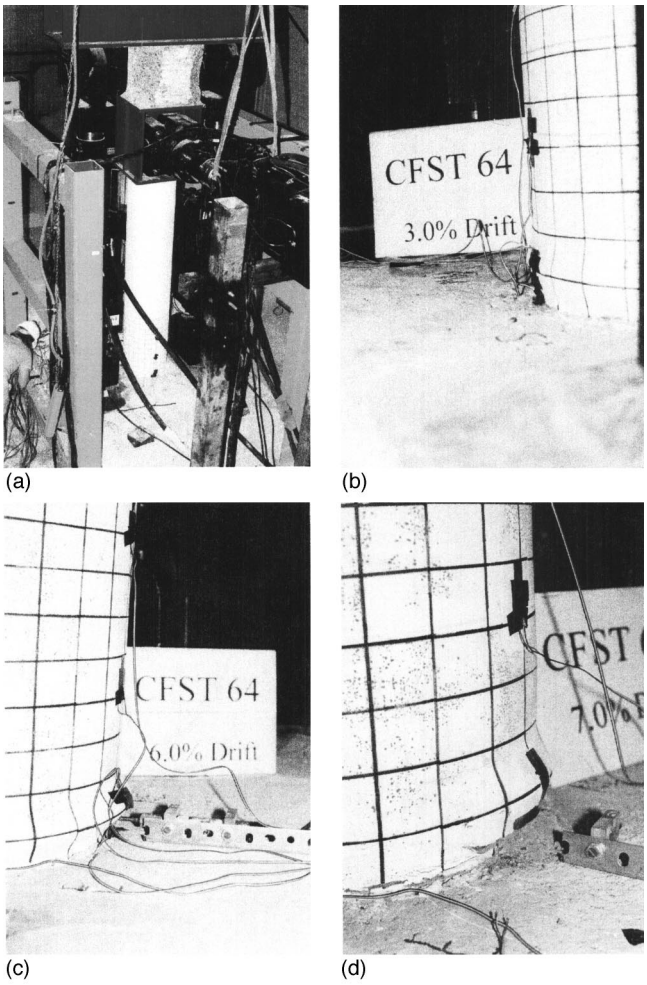

Fig. 5. CFST 64 (a) test setup; (b)–(d) local buckling at 3, 6, and 7% drift (with fracture at 7% drift)

CFST 34

The force–deflection results obtained during testing is shown in Fig. 4. Behavior remained essentially elastic until the third prescribed set of three loading cycles ($0.75\delta_y$), when some strain gauges indicated strains just below the yield strain. Deviation of the force–displacement relationship from the elastic line also began to be noticeable. At a displacement of 22 mm, strain gauges started to indicate values greater than the yield strain, and there was deviation of the force–displacement curve from the elastic line. It was decided to define the effective δ_y at 1% drift. Small longitudinal cracks in the paint were visible on the south east side from the base of the concrete foundation to the middle of the second grid line during the second positive cycle at 1.0% drift. A very small buckle became visible on the west and east side of the column during the second cycle at 3% drift for positive and negative forces, respectively (Fig. 6). A maximum load of 190 kN was reached at a deflection of 3% drift and the specimen continued to resist this load until the first cycle at 7% drift. During the first negative cycle at 4% drift, the east buckle did not straighten out completely and the west buckle did not straighten out completely during the second positive cycle at 4% drift. During cycling at 5 and 6% drift, the buckles continued to grow. At 7% drift, the buckle around the column had become quite significant (Fig. 6). After the second cycle had been completed at 7% drift and no cracking was observed, it was decided to attempt cycles at 8%

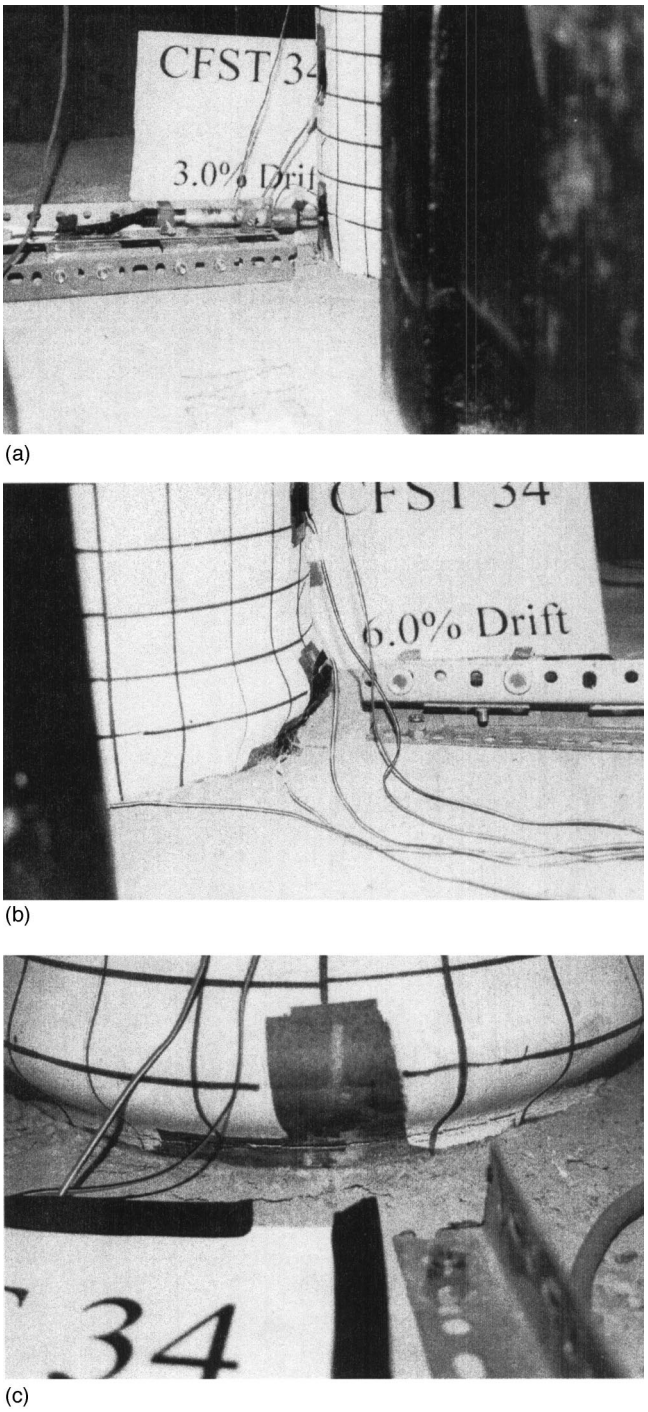

Fig. 6. CFST 34 (a)–(c): buckling at 3, 6, and 7% drift (with fracture at 7% drift)

drift. Unfortunately, readings from temposonic LVDT 1 were lost while loading to negative 8% drift (the point of maximum retraction of the horizontal actuator). It was also discovered at that point that during loading at 6 and 7% drifts a deficiency in the experimental setup prevented the smooth movement of the temposonic guide bar through its circular magnet. This added friction resulted in jaggedness in the shape of the force–deflection diagram and contributed to the loss of reliable readings. Upon discovery of this problem, the test was stopped, the horizontal actuator was returned to its zero starting position, and the vertical actuators were unloaded. The strain gauges on the east and west sides just above the foundation were removed to ascertain damage to the column. Longitudinal cracks on both the east and the west sides were found approximately 2 mm up the column from the top of the concrete foundation and were estimated to be approximately 1 mm deep.

The test was restarted by loading each of the vertical actuators with 960 kN of force. Cyclic horizontal displacements were applied anew at 7% drift. During second positive cycle, miniature, transverse cracks were visible on the east side. At the second negative cycle, buckling had increased on both the east and west sides. The transverse cracks on the east side joined together and the buckle on the west side pointed down instead of perpendicular to the column. Failure on the west side occurred when a large crack developed in the buckle and penetrated the steel during the third positive cycle. The 25 mm crack opened up on the top of the first grid line, to a crack width of 3 mm. Failure on the east side occurred during the third negative cycle when a transverse crack on the bottom of the buckle penetrated the steel tube. The 140-mm-long crack had a height of 9 mm. Testing stopped. Upon final inspection, a smaller crack was observed above the buckle on the east side after unloading.

CFST 42

The experimentally obtained hysteretic force–displacement behavior is shown in Fig. 4. This column had the largest predicted moment resistance. As for the previous tests, significant yielding had not occurred when first departure from the elastic line of the force–displacement curve was observed at 15 mm ($0.75\delta_y$). Yielding in some strain gauges on the steel tube and departure from the elastic line occurred at 22 mm drifts, and, at this displacement, the deflection was deemed to be equal to δ_y, which also coincided with 1% drift. During the third negative cycle at 1% drift, a small opening on the foundation against the east side of the column was found. A very slight buckle was seen on the east side between the first and second grid line during the first positive cycle at 2% drift. During the second negative cycle at 2% drift, a slight decrease in strength was noticed in the force versus deflection diagram. However, no buckling could be seen. During the third cycle at 2% drift, the gap between the column and the concrete foundation widened.

A maximum horizontal force of 400 kN was reached while cycling at 3% drift, and the specimen was able to resist this load until the end of cycling at 5% drift. The buckle on the east side had become more pronounced at 3% drift (Fig. 7); it started at the third grid line and ended at the top of the concrete foundation. It appeared to be at a maximum where the LVDT was situated. During the third negative cycle at 3% drift, the buckle was visible on the west side. The gap between the column and the foundation was measured to be 2 mm wide and grew during cycling at 4% drift. The buckles on both sides of the column continued to grow during 4% drift. The west side buckle did not straighten out during the first cycle at 5% drift. At the end of cycling at 5% drift, no visible cracks were visible near either buckle. The column, however, appeared to be leaning slightly to the north, but there was no evidence of twisting. The buckle had grown to encompass the entire diameter of the column but appeared to be more pronounced on the north than on the south side.

During cycling at 6% drift, no cracks could be seen but the buckles on both sides had grown. During the second cycle at 7% drift, small hairline cracks on the west and east sides could be seen. Cracking developed around the buckle, and necking of the steel shell was observed during the fourth negative cycle on the west side. On the reverse cycle, the cracks began to join and

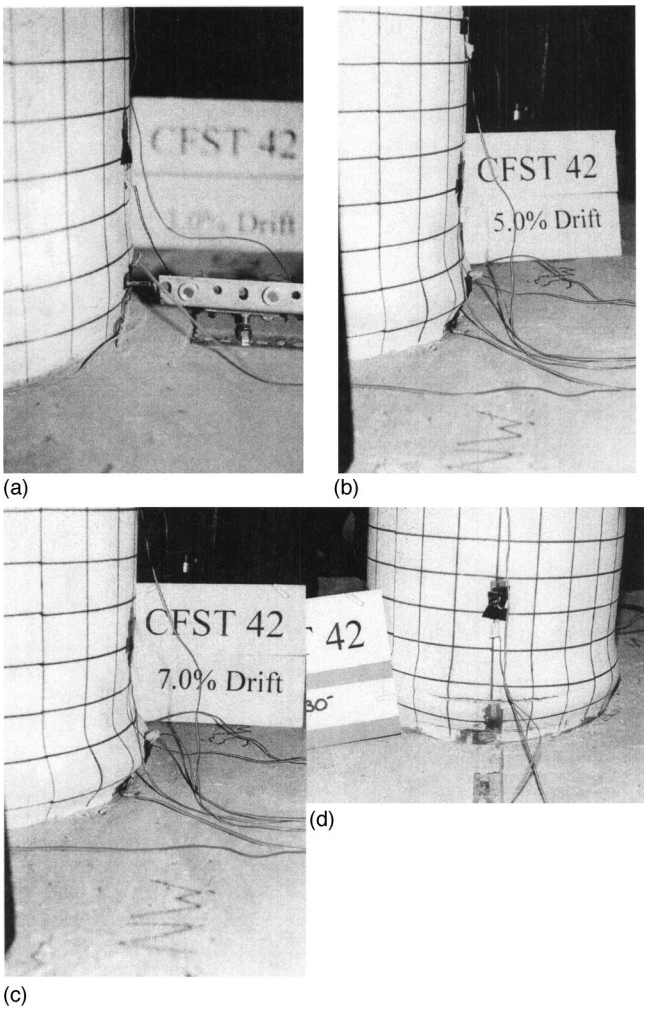

Fig. 7. CFST 42 (a)–(c): local buckling at 3, 5, and 7% drift (with fracture at 7% drift); (d) specimen after 30 cycles

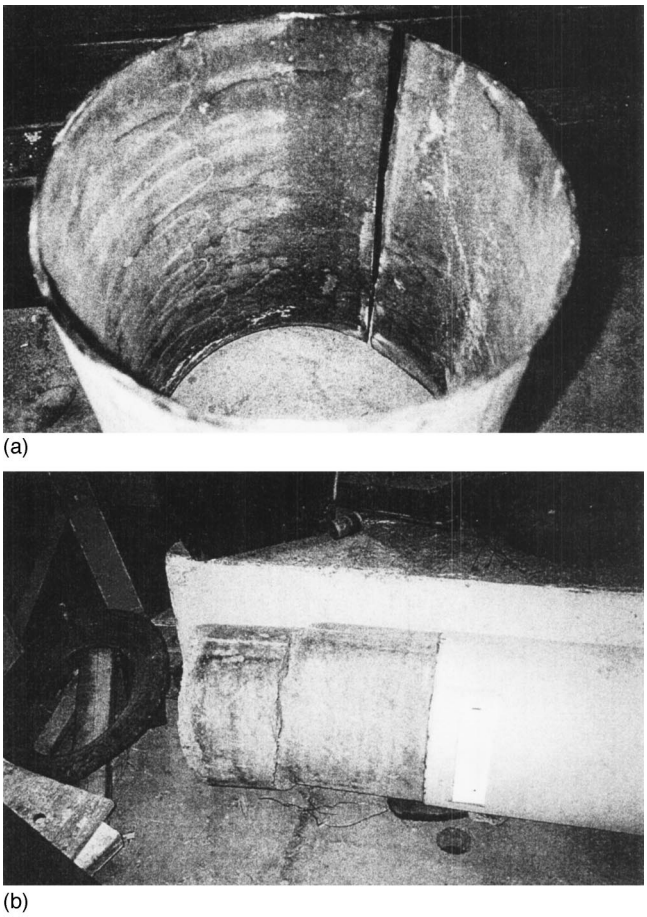

Fig. 8. (a) Steel section after removal from column; (b) column and concrete after removal of steel section

necking occurred in the middle of the east side buckle (Fig. 7). A bang was heard as the crack in the middle of the west buckle suddenly propagated to a length of 260 mm and fractured the steel shell. The load dropped to 60 kN at the sixth positive cycle. At the sixth negative cycle, another bang occurred and the crack in the middle of the east side buckle similarly propagated to a length of 233 mm and fractured the steel. Testing stopped. Cracks on the bottom of the buckle on both the west and east sides had not penetrated the steel.

CFST 51

The experimentally obtained hysteretic force–deflection results are shown in Fig. 4. Contrary to the previous tests, after the third negative cycle at 0.75% drift, a very slight buckle was seen on the west side of the column. However, there was still no deviation of the force–displacement curve from the elastic straight line at this time, and no strain gauges on the steel tube indicated yielding. Therefore, the specimen was deemed to still be below the effective yield displacement. Similar to the previously tested specimens, observed data supported the effective yield displacement at 22 mm, corresponding to 1% drift. A small opening was visible on both the east and west sides of the column between the steel tube and the concrete foundation during the third cycle at 1% drift. A slight buckle began to develop on the east side during the first cycle to 2% drift. Pinching of the force–displacement curve during the second negative cycle at 2% drift suggested that buckling was occurring somewhere in the steel tube. Upon closer examination the buckle on the west side was visible. Further cycling at 2% drift produced a larger gap at the steel tube and concrete foundation interface.

A maximum applied horizontal force of 155 kN was reached during cycling at 3% drift. The east side buckle became more significant by the first cycle to 3% drift and continued to grow during cycling at 3% drift, however, the buckle on the west side was smaller in comparison to the buckle on the east side. The buckle on the east side completely straightened out upon load reversal until the second negative cycle at 4% drift while the buckle on the west side fully straightened out upon such reversal until the first positive cycle to 5% drift. During cycling at 4 and 5% drifts, the buckles on both sides grew and the buckle became visible around the entire circumference. However, no cracks were seen. The column leaned to the south slightly, and the buckle on the south side was, typically, larger than on the north side.

Vertical cracks became visible on top of the buckle on the west side during the first negative cycle at 6% drift. After reversing the load, vertical cracks were seen on the northeast side of the buckle and the vertical cracks on the west side had completely closed up. The buckle on the southwest side began to droop and point down. During the first cycle at 7% drift, the buckle on the east side also began to droop and point down instead of developing perpendicular to the column. The negative cycle produced horizontal cracks

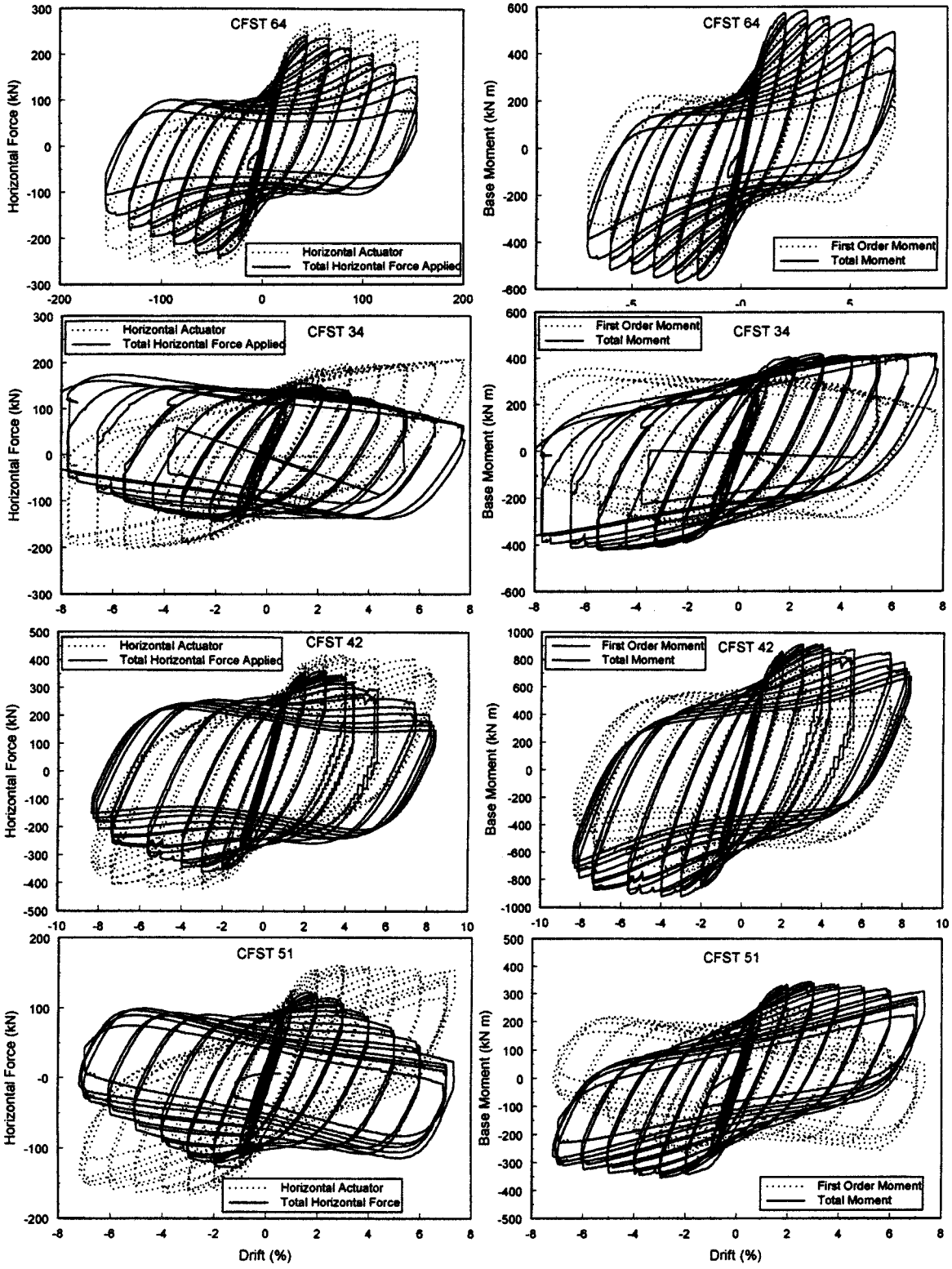

Fig. 9. Force–displacement curves with and without $P-\Delta$ corrections

on the bottom and top of the buckle on the east side. During the next cycle, the horizontal and vertical cracks began to penetrate the thickness of the steel shell. The vertical cracks had completely opened up on the east side during the fourth positive cycle. Also, on the east side, a transverse crack was noticed in the middle of the buckle, while necking had started on the buckle on the west side. After the next load reversal, the fourth negative cycle of 7% drift, a bang was heard and a through thickness fracture occurred in the middle of the buckle on the east side. The length of the crack was 220 mm and its width was 20 mm. The vertical cracks had penetrated through the thickness of the steel and necking became severe on the west side. Another loud bang was heard during the fifth positive cycle at 7% drift when fracture occurred along the center of the buckle on the west side. The crack length

was 160 mm and the width was 13 mm. On the east side, twovertical cracks had completely penetrated the steel. The test was stopped at this point.

Bond

To dispose of the specimens, one cut was made below the buckle on the steel tube. The column was then lifted off of the foundation. The concrete at this location was very weak and offered no resistance when the column was removed. Upon closer examination of the foundation, the concrete remaining in the steel tube was pulverized at the interface but quite cohesive and intact just below the foundation. This suggests that only the concrete behind the buckle experienced crushing while the remaining concrete core, above and below the buckle did not crush or fail.

Although not a primary objective in this study, an investigation of the bond remaining after testing was conducted on specimen CFST 51 before it was disposed. A circumferential cut was made, approximately 560 mm above the foundation. The bottom cut was made above the buckle, approximately 90 mm above the foundation. A vertical cut was made between these two horizontal lines. The column was then lifted off of the foundation. While still being supported, the column stood vertically on the ground. The column was tapped twice and the cut section fell off of the concrete core. The steel tube and the remaining column is shown in Fig. 8. The origin of the crack in the concrete core is not known, however, it is suspected that it was caused by the removal of the steel tube section. There were no signs of concrete cohesion on the steel tube. No concrete residue was left on the steel tube and the concrete core looked smooth. However, there was some white dust on the inside of the steel tube verifying that no significant concrete shrinkage occurred. The full bond strength was not retained at the end of testing for this column. This investigation was very limited and only looked at the bond after complete failure of both the steel and concrete.

Other Issues

Analysis of test results, using information from the strain gauges positioned on the steel tube, showed that, in all cases, the maximum moment along the concrete-filled columns generally occurred below and near the top of the concrete foundation (at most, 100 mm into the concrete foundation). The strain gauge results also indicated that the steel sections used in the foundation (other than the tube itself) were subjected to insignificant stresses, suggesting that the concrete foundation likely provided most of the resistance to the composite moment.

Finally, note that $P-\Delta$ effects on the four tested specimens were significant, as revealed by the hysteretic curves corrected for $P-\Delta$ effects shown in Fig. 9. These effects must be considered in analysis.

Conclusions

Four concrete-filled steel tubes were subjected to both an axial load and a cyclic bending moment. The diameters of these columns were 324 and 406 mm, with a D/t ratio ranging from 34 to 64. All columns were embedded in a special foundation detailed to develop the full plastic moment from the composite column. Experimental work shows that:

- The ductility of all tested columns was good, all columns being able to reach drifts of 7% before a significant loss in moment capacity occurred as a result of cracks opening on the local buckles.
- The maximum flexural strength of all columns was reached at approximately 4% drift.
- Strength deterioration after the maximum strength was reached was slow until fracture occurred during cycling at 7% drift.
- The favorable hysteretic curves produced from the tests showed good energy dissipation for all columns.
- The foundation detail worked well, ensuring that full moment resistance capacity of the concrete-filled steel column could be developed during testing (data show that the proposed foundation detail could be significantly optimized).
- No significant bond was seen between the steel tube and the concrete core after testing had been completed.

These experimentally obtained results suggest that concrete-filled steel circular tubes could provide an effective mechanism to dissipate seismic energy. As such, they could provide a viable alternative for bridge piers in seismic regions of North America, at least up to the column sizes tested in this study. Future research will permit us to significantly reduce the foundation sizes, better understand details of the behavior, and investigate whether larger columns would exhibit the same good behavior.

Acknowledgments

This research program was funded by the Natural Science and Engineering Research Council of Canada and the Structural Steel Education Foundation. This support is sincerely appreciated. However, the opinions expressed in this paper are those of the writers and do not reflect the views of the aforementioned sponsors.

References

Alfawakiri, F. (1997). ''Behavior of high strength concrete-filled circular steel tube beam columns.'' MS thesis, Univ. of Ottawa, Ottawa.

American Association of State Highway and Transportation Officials (AASHTO). (1994). ''LRFD bridge design specifications.'' Washington, D.C.

Applied Technology Council (ATC). (1992). ''Guidelines for cyclic seismic testing of components of steel structures.'' *Rep. No. ATC-24*, Redwood City, Calif.

Bauer, C. J. (1988). ''New standards for innovative composite construction.'' *Constr. Specifier*, 04, 84–89.

Boyd, P., Cofer, W. F., and McLean, D. E. (1995). ''Seismic performance of steel-encased concrete columns under flexural loading.'' *ACI Struct. J.*, 92(3), 355–364.

Bruneau, M., and Marson, J. (2004). ''Seismic design of concrete-filled circular steel bridge piers.'' *J. Bridge Eng.*, 9(1), 24–34.

Canadian Standards Association (CSA). (1994). ''Limit states design of steel structures—CAN/CSA-S16.1-94.'' Rexdale Ont., Canada.

Canadian Standards Association (CSA). (2000). ''Canadian highway bridge design code—CAN/CSA-S6-00.'' Rexdale Ont., Canada.

Kerensky, O., and Dallard, N. (1968). ''The four-level interchange between M4 and M5 motorways at Almodsbury.'' *Proc. Inst. Civ. Eng., Struct. Build.*, 40, 295–322.

Kitada, T. (1992). ''Ductility and ultimate strength of concrete-filled steel members.'' *Stability and ductility of steel structures under cyclic loading*, U. Fukumoto and G. Lee, eds., CRC Press, Boca Raton, Fla., 139–148.

Knowles, R. B., and Park, R. (1969). ''Strength of concrete filled steel tubular columns.'' *J. Struct. Div. ASCE*, 95(12), 2565–2586.

Marson, J., and Bruneau, M. (2000). ''Cyclic testing of concrete-filled circular steel bridge piers having encased fixed-based detail.'' *Ottawa Carleton Earthquake Eng. Res. Center, Rep. No. OCEERC 00-22*,

Univ. of Ottawa, Ottawa.
MTO. (1991). *Ontario highway bridge design code*, 3rd Ed., Ministry of Transportation, Government of Ontario, St. Catherines, Ontario, Canada.
Prion, H., and Boehme, J. (1994). ''Beam-column behavior of steel tubes filled with high strength concrete.'' *Can. J. Civ. Eng.*, 21(2), 207–218.
Tarics, A. G. (1972). ''Concrete-filled steel columns for multistory construction.'' *Modern Steel Constr.*, 12, 12–15.
Viest, I. M., Colaco, J. P., Furlong, R. W., Griffis, L. G., Leon, R. T., and Wyllie, L. A., Jr. (1997). *Composite construction design for buildings*, American Society of Civil Engineers and McGraw-Hill, New York.
Vogeli, R. (1950). ''New transmission lines with concrete filled steel tube towers.'' *Proc., Int. Conf. Large Electric Systems*, 2(223).
Webb, J., and Peyton, J. M. (1990). ''Composite concrete-filled steel tube columns.'' *Proc., 2nd Natl. Structures Conf.*, The Institution of Engineers, Adelaide, Australia, 181–185.